Molecular Beam Laser-Induced Fluorescence Studies of Chemical Reactions

Crossed molecular beam experiments that use laser-induced fluorescence spectroscopy as the detector allow measurements of the internal state distribution in the products of chemical reactions studied under well-controlled single-collision conditions. This technique provides direct information on the chemical dynamics and the intermolecular potential surfaces. Application to the reactions $H + NO_2 \rightarrow OH + NO$ and $O(^3P) + C_6H_{12} \rightarrow OH + C_6H_{11}$ is discussed where the OH state distribution has been measured.

Introduction

An age-old goal in chemistry is to understand the nature of those forces involved in the making and breaking of chemical bonds, *i.e.*, the forces that drive chemical reactions. Despite the maturity of chemistry, this understanding is still in its infancy.

For many years chemical kinetics has been spectacularly successful in identifying elementary reactions and in measuring their rates under conditions of thermal equilibrium. Such measurements are essential for the understanding of reaction mechanisms and for kinetic modeling of complex chemical environments, e.g., in combustion or atmospheric chemistry. However, the rate constant is a macroscopic property of the reaction and represents an average over all possible collisions of the reactants. It has, therefore, been difficult to extract directly information on the chemical forces from such kinetic measurements.

In contrast, chemical dynamics attempts to view the reaction at its most fundamental microscopic level, e.g., as the outcome of an individual collision or scattering between two reactant molecules. Properties of the reaction measured under such single-collision conditions reflect much more directly the chemical forces [1]. The resurgence of interest in chemical dynamics over the past twenty years is principally due to the development of the crossed molecular beam scattering technique. Thus, for the first time, the properties of chemical reactions can be measured under this single-collision condition. These

scattering experiments involve the intersection of two molecular beams in a small localized volume, where at most a single collision occurs between the two reactants. If the collision leads to a chemical reaction, the product molecule may be detected by a particle detector such as a mass spectrometer. Interest in these experiments has centered on measurements of the angular distribution of product molecules formed in the reaction, from which the detailed kinematics of collisions, lifetimes of collision complexes, and geometries of transition states can be inferred. More refined experiments with velocity analysis of the products and velocity selection of the reactants provide information on the role of translational energy in the reaction: the fraction of exothermicity released as translational energy, the dependence of cross section on reactant velocity, and the coupling between scattering angle and product velocity. Recent experiments of this type have been covered in excellent reviews [2].

Although molecular beam experiments with particle detectors provide unique information on chemical reactions that is unobtainable by any other means, the technique still has serious limitations. First, the experiments represent a considerable technological undertaking, primarily because of the need for sensitive and low-background mass spectrometers to detect the very low flux of product molecules. A more fundamental limitation is the inability of the particle detector to resolve the internal states of the product. Various purely spectroscopic techniques, such as infrared chemiluminescence and chemical laser gain

Copyright 1979 by International Business Machines Corporation. Copying is permitted without payment of royalty provided that (1) each reproduction is done without alteration and (2) the *Journal* reference and IBM copyright notice are included on the first page. The title and abstract may be used without further permission in computer-based and other information-service systems. Permission to *republish* other excerpts should be obtained from the Editor.

measurements, can be used in favorable cases to determine the nascent product state distribution for the reaction, but not under the carefully controlled collision conditions of the molecular beam experiment.

Clearly, the ideal chemical dynamics experiment is a marriage between spectroscopic and molecular beam techniques, e.g., the use of absorption spectroscopy as the detector in a crossed molecular beam experiment. However, the density of product molecules formed in crossed beam reactions is extremely low, typically $\approx 10^6/\text{cm}^3$ in the collision zone where the two beams intersect and $\approx 10^4/\text{cm}^3$ in regions away from the collision zone (where a scan of the angular distribution is possible). Obviously, such densities are orders of magnitude too low to apply normal absorption spectroscopy as the detector. Schultz et al. [3] first pointed out that laser-induced fluorescence (LIF) spectroscopy indirectly measures the absorption spectrum of a molecule and is sensitive enough to detect the products of crossed molecular beam chemical reactions.

In essence, the LIF technique consists in scanning a tunable laser through an electronic absorption band of the product molecule. When a specific transition between definite internal levels is encountered, a fraction of those in the level of the ground electronic state is transferred to the excited electronic state. Once there, they can fluoresce and the total fluorescence can be detected very sensitively. If the radiative properties of the product are known, the absorption spectrum can be obtained from the relative intensities of the excitation spectrum.

Schultz et al. [3] have detected $\approx 5 \times 10^4$ BaO molecules per quantum state per cm³, and Mariella et al. [4] have detected ≈20 OH molecules per quantum state (a density of $\approx 5 \times 10^3$ OH molecules per quantum state per cm³). This sensitivity is comparable to that obtainable with mass spectrometers, but it now has quantum state resolution. However, with LIF the total product density must now be approximately one to two orders of magnitude greater than with mass spectrometers since each quantum state is detected individually. The LIF sensitivity is currently limited only by the available lasers. For example, pulsed tunable dye lasers at ≈ 10 pulses per second are now most commonly used for LIF; future development of higher-repetition-rate lasers could increase the ultimate sensitivity of LIF by two to three orders of magnitude.

Since a large excess of reactants does not affect the spectroscopy of the product, LIF is in general immune to the background problems associated with mass spectrometric detectors. This significantly reduces the vacuum

requirements and thus the technological burden associated with molecular beam experiments.

The advantages of LIF are obtained, however, at the price of the technique's generality because of stringent conditions for its applicability. The product must have a strong electronic absorption in the region of presently available tunable lasers (\approx 260-700 nm). The detailed spectroscopy and radiative properties of the products must be already well characterized. Finally, the quantum yield for fluorescence in the excited electronic state must be nearly one. This last condition generally limits LIF detection to some diatomic and a few triatomic molecules. The OH radical is particularly well suited to LIF detection. The single disadvantage of OH is that only rotational levels $K \le 25$ in v = 0 and $K \le 18$ in v = 1 can be observed because of predissociation in the $^2\Sigma$ state [5].

Laser-induced fluorescence has now been used as the detector in several crossed molecular beam experiments, principally to measure the internal state distribution of the products [6]. Second-generation LIF experiments are just beginning; *e.g.*, simultaneous vibrational and angular scattering distributions [7] have now been obtained. The effects of initial translational energy [8], reactant vibration [9], and reactant orientation [10] on the product state distribution have also been observed.

We report the application of LIF to measure the nascent OH product state distribution under crossed molecular beam conditions for two very dissimilar chemical reactions, $H + NO_2 \rightarrow OH + NO$ and $O(^3P) + C_6H_{12} \rightarrow OH + C_6H_{11}$. For the reaction of $H + NO_2$, the effects of reactant rotation were investigated; for the reaction of $O(^3P)$ with cyclohexane, the effect of initial translational energy was investigated. Such measurements yield direct information on the dynamics and intermolecular potentials of the reactions.

Experimental method

A schematic diagram of our crossed molecular beam scattering apparatus with LIF detection of products is shown in Fig. 1. Details of the experiment have been reported elsewhere [4]; only a brief description is given here. The apparatus includes a hydrogen or oxygen atomic beam source generated by either an rf or microwave discharge in the parent gas. This source produces a beam of thermal atoms at \approx 340 K, with dissociation efficiencies of \approx 95% for H_2 and \approx 30% for O_2 . The other reactant beam is either a simple effusive beam or a supersonic nozzle beam [11]. The nozzle beam causes substantial cooling of the gas through hydrodynamic expansion in both the internal states and the velocity distribution of the reactant. The nozzle beam also allows the reactant to be translationally

597

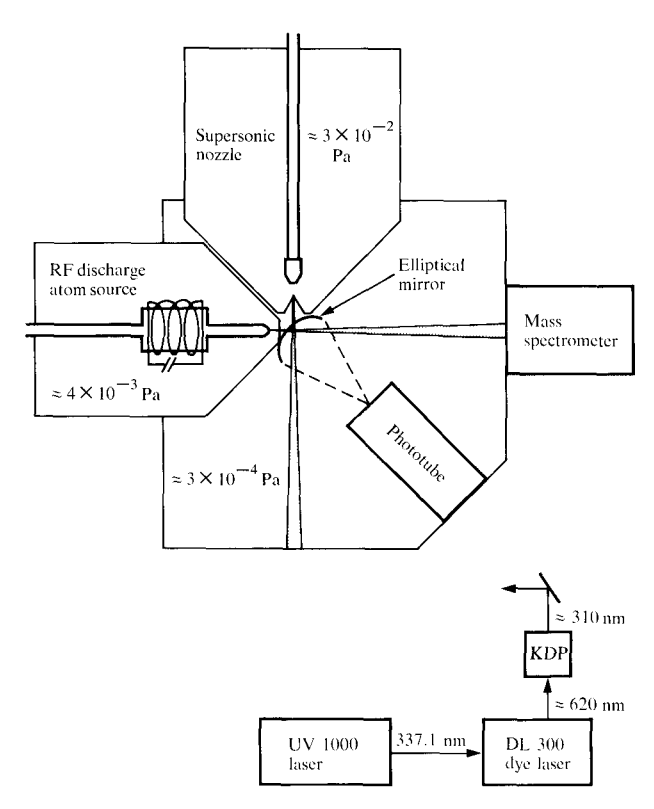


Figure 1 Schematic of the crossed molecular beam scattering apparatus with laser-induced fluorescence detection.

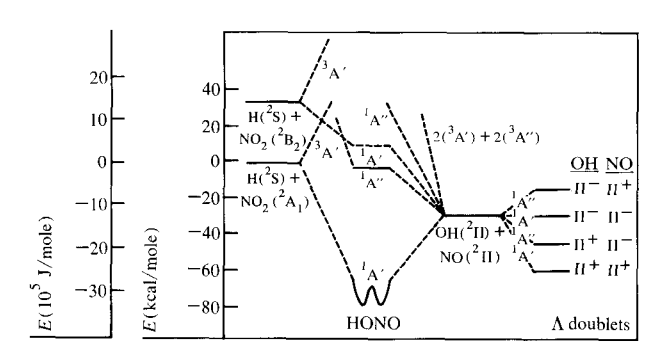


Figure 2 Schematic correlation diagram for the reaction H + $NO_2 \rightarrow OH + NO$, assuming C_s symmetry.

accelerated by "seeding" it in an excess of a light carrier gas [11]. This is essential for the O(³P) plus saturated hydrocarbon reactions since they have substantial energy barriers to reaction. A quadrupole mass spectrometer is used to monitor the beams separately or in combination with a chopper, allowing the beam velocities to be measured through their time of flight.

The laser detection system consists of a Molectron DL 300 (Molectron Corp., Sunnyvale, CA) dye laser pumped

by a Molectron UV 1000 nitrogen laser. The output of the dye laser is frequency-doubled to provide tunable radiation in the ultraviolet from about 257 to 345 nm with ≤ 10 - μ J pulses, a linewidth of 1 to 2 cm⁻¹, and at a repetition rate of ≈ 10 pulses per second. The laser beam, which is directed perpendicularly to the plane of Fig. 1 and toward the scattering zone, enters the chamber through a series of optically collimating baffles and excites OH in the $^2\Sigma \leftarrow ^2\Pi$ transition. An elliptical mirror surrounds the scattering center and images $\approx 50\%$ of the total OH laser-induced fluorescence onto a photomultiplier.

Results and discussion

$\bullet \ H + NO_2 \rightarrow OH + NO$

This reaction is very familiar in chemical kinetics since it is the standard laboratory source of OH. It has a large thermal rate constant at 300 K, with little or no barrier to reaction [12]. Since a weak NO bond is broken and a stronger OH bond is formed, the reaction is exothermic, with $\Delta H = -29.5$ kcal/mole (-1.24 × 10⁵ J/mole). When the reaction occurs in an argon matrix at 4-14 K, HONO is isolated, rather than the diatomic products [13]. This suggests, but does not conclusively prove, that the reaction proceeds through formation of a HONO complex. The molecular beam scattering data presented in this paper also indicate such a reaction mechanism. The correlation diagram of Fig. 2 provides the qualitative features of the potential surface. Most important are the potential minima representing HONO, which are ≈50 kcal/mole $(2.1 \times 10^5 \text{ J/mole})$ stable with respect to the products. The total energy available for the reaction is ≈30 kcal/mole $(\approx 1.3 \times 10^5 \text{ J/mole})$ more than the OH + NO dissociation energy for this complex. In the matrix reaction, the matrix dissipates the excess energy and allows the HONO complex to be stabilized. In the gas phase, however, no means exist for an isolated HONO molecule to dissipate this energy before dissociation occurs.

The reaction looks very much like a chemical activation process, *i.e.*, a highly vibrationally excited HONO is formed, which ultimately undergoes unimolecular decay to products. Simple RRKM (Rice-Ramsperger-Kassel-Marcus) estimates [14] suggest that the HONO complex lives for $\approx 5 \times 10^{-12}$ s, or ten to fifteen vibrational periods. If the lifetime of a collision complex is long enough, it has no memory of the way in which it was formed, except for the conservation of total energy and total angular momentum. In this case the complex decays statistically, governed only by the final density of states.

Crossed molecular beam experiments with a particle detector [15] have shown that the angular distribution of products from this reaction is almost isotropic in the cen-

ter-of-mass coordinate system. This is consistent with statistical scattering from a complex with a lifetime of $\approx 5 \times 10^{-12}$ s. Here, we report the measurement of rotational and fine structure partitioning into the OH product and show that the results are not consistent with a statistical model; details are presented in Ref. [4].

With a thermal beam of NO_2 as the reactant, primary energy disposal into the product OH has been measured by using the techniques outlined previously. The rotational state (K) dependence of the reactive cross sections is a rather undistinguished broad single maximum for each vibrational state of OH and peaks at $K \approx 16$ for v = 0 and $K \approx 12$ for v = 1. The K dependence of the cross sections has been analyzed using Levine-Bernstein surprisal theory [16]. Surprisal theory compares the observed internal state distribution to that expected statistically. The surprisal is defined as

$$I(J|v, E) = -\ln \left[\frac{P(J|v, E)}{P^{0}(J|v, E)} \right],$$

where P(J|v, E) and $P^{0}(J|v, E)$ are the experimental and statistical rotational state distributions, respectively, for the vibrational level v. A horizontal line in such a plot means that the observed distribution is statistical. The application of surprisal theory to our results is given in Fig. 3. Large rotational surprisals are obtained for each vibrational state. Further, this rotational surprisal is nearly independent of the vibrational state, as suggested by Levine and Bernstein [17]. The curvature for low rotational states in this plot is probably due to a rotationally relaxed background of OH in the scattering chamber. This background arises both from OH produced in the atom source and from a small fraction of the OH product that has partially relaxed through collision with the walls of the chamber. In contrast to most previous studies where rotational surprisals have been small, this reaction produces considerably more rotational excitation of OH than is predicted statistically. Our results agree qualitatively but not quantitatively with previous measurements by Silver et al. [18].

One intriguing aspect of the dynamics is the source of the large rotational excitation of OH. It could be a consequence of the rotation of the NO_2 reactant, namely, to conserve angular momentum. (In these experiments, a thermal beam of NO_2 was used as the reactant, and the NO_2 was rotationally excited with a broad Boltzmann distribution of rotational states peaking at $J_{NO_2} \approx 25\hbar$.) To investigate this possibility, energy partitioning into OH has been measured using as the reactant a supersonic nozzle beam of 10% NO_2 seeded in argon. In this case the NO_2 is translationally and rotationally cooled, with a translational temperature of 8 K as measured by time-of-

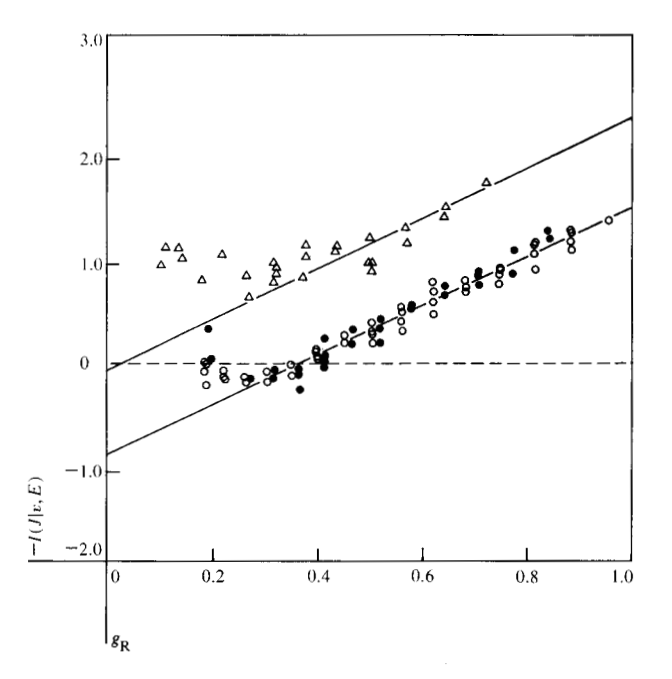


Figure 3 Rotational surprisals for OH produced in the crossed molecular beam reaction $H + NO_2 \rightarrow OH + NO$. The \bigcirc indicate results for v = 0 and the \triangle for v = 1 OH where the reactant rotation $J_{NO_2} \approx 25\hbar$. The \blacksquare indicate results for v = 0 OH and $J_{NO_2} \approx 4\hbar$. Each data point corresponds to a different rotational transition. For the purposes of this plot, the points for Q-branch transitions have all been scaled by a single constant to eliminate effects due to nonstatistical fine structure partitioning. The solid lines are the best-fit linear surprisals. I(J|v, E) is the rotational surprisal for the state (J, v); $g_R = E_R/(E - E_V)$, where E_R is the rotation energy of state (J, v), E_V is the vibrational energy of the state (J, v), and E is the total reaction energy.

flight experiments on the velocity dispersion of the beam. Smalley et al. [19] have shown that under nozzle conditions similar to those used here, rotational cooling for NO Ar beams lags only slightly behind translational cooling. We estimate the rotational temperature for our beam as \approx 12 K ($J_{NO_2} \approx 4\hbar$). The velocity of NO₂ in the nozzle beam is nearly the same as the average velocity of NO_a from the thermal beam. Thus, the collision energy is not significantly changed. A comparison of the rotational surprisals for the v = 0 OH results for the two levels of reactant rotation (also shown in Fig. 3) indicates no difference in the rotational partitioning. This clearly demonstrates that the energy disposal and the large rotational excitation of OH are insensitive to that part of the potential surface defining the entrance channel. These effects are probably governed by that part of the surface corresponding either to breakup of the collision complex or to the exit channel.

We can gain further insight into angular momentum partitioning from the nozzle results by simply considering the requirement for conservation of angular momentum:

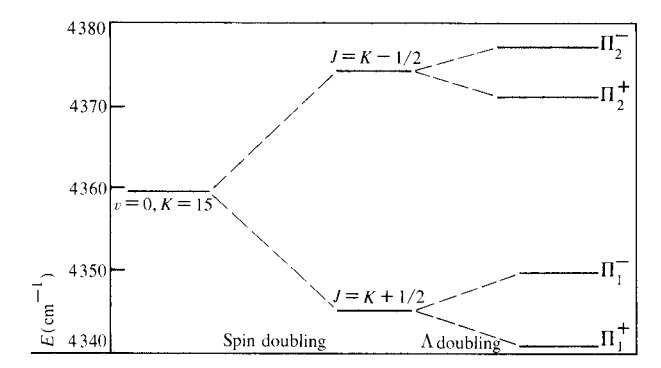


Figure 4 Typical fine structure splittings in a rotational level of $OH(^2\Pi)$.

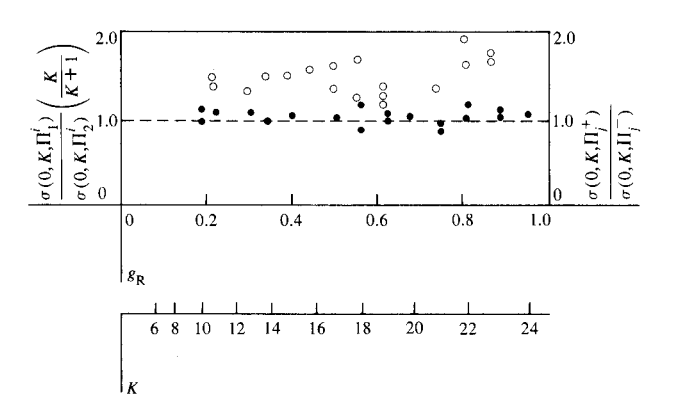


Figure 5 Observed fine structure partitioning for rotational levels of v=0 OH produced in the chemical reaction $H+NO_2 \rightarrow OH+NO$; K is the rotational quantum number and σ is the observed cross section; $i=\pm$ and j=1,2. The horizontal line at 1.0 is the statistical result. The \bullet are for the partitioning into spin doublets (left axis); the \bigcirc are for partitioning into Λ doublets (right axis).

$$\vec{L} + \vec{J}_{NO_{\alpha}} = \vec{L}' + \vec{J}_{OH} + \vec{J}_{NO} , \qquad (1)$$

where \vec{L}' is the product orbital angular momentum and \vec{J}_{NO_2} , \vec{J}_{OH} , and \vec{J}_{NO} are the respective internal molecular angular momenta. The value of the reactant orbital angular momentum \vec{L} can be estimated to be $\leq 2\hbar$ from the total reactive cross section $(2\times 10^{-16}~\text{cm}^2)$. Since there is no barrier in the exit channel, L' can be estimated from the usual requirement of passage over a centrifugal barrier, i.e., $L' \leq 12\hbar$ [20], $J_{\text{NO}_2} \leq 4\hbar$, and $J_{\text{OH}} \leq 24\hbar$ (as measured); we have no direct information on J_{NO} . However, to conserve angular momentum, NO must also be substantially rotationally excited for high J_{OH} states. Furthermore, \vec{J}_{NO} must be preferentially aligned antiparallel to \vec{J}_{OH} . In fact, the rotation in NO is approximately equal in magnitude but oppositely directed to that of OH.

Spin-orbit and orbital-rotation interactions in ²Π radicals such as OH cause fine structure splittings for each rotational level (see Fig. 4). Since each of the fine structure levels can be probed by different rotational subbands, i.e., Π_1^+ by P_1 or R_1 , Π_1^- by Q_1 , Π_2^+ by P_2 or R_2 , and Π_{2}^{-} by Q_{2} [21], relative cross sections for production of each of the sublevels may be determined separately. The fine structure splittings are negligible compared to the reaction energy ($\approx 30 \text{ kcal/mole}$ or $\approx 1.3 \times 10^5 \text{ J/mole}$); thus, we would not expect any selectivity in the filling of these levels (statistical partitioning). Observed results for rotational levels in v = 0 OH using the thermal NO_a source as a reactant are given in Fig. 5. It is clear that the spin doublets are produced statistically, but there is a substantial preference for the Π^+ Λ -doublet component. This propensity,

$$\frac{\sigma(\Pi^+)}{\sigma(\Pi^-)} = 1.5 \pm 0.2,$$

is approximately independent of the vibrational and rotational levels produced in the reactive scattering. A brief account of this is presented in Ref. [22].

The physical difference between the two Λ -doublet components Π^+ and Π^- lies in the orientation of the electron density of the singly occupied OH π orbital relative to the plane of rotation of the molecule. For high rotational states, this electron density forms lobes either in the rotation plane or perpendicular to it (Fig. 6) [23, 24].

Partitioning into final quantum states is determined principally by the breakup of the HONO collision complex. The singly occupied OH π orbital essentially points along the direction of the NO bond that is broken during the course of the reaction. A Π^+ state of OH is formed when the reaction generates a torque in a plane containing this bond, while the Π^- state results when the reaction generates torques about this bond. Our experiments show that the principal reactive trajectories lie in a plane containing the NO bond, *i.e.*, that the overall reaction occurs in a plane.

The correlation diagram for this reaction in the planar geometry (given in Fig. 2) is an approximate representation of the surface. In this figure, the regions given as solid lines are supported by experimental data, while the regions given as dashed lines represent reasonable speculations about the surface. As discussed, the reaction is thought to proceed through the lowest ¹A' surface that includes the HONO complex.

 $Ab\ initio$ calculations on NO_2 show that the unpaired electron in the 2A_1 state of the radical is essentially localized in a planar approximately sp^2 hybrid orbital on the

nitrogen [25]. Chemical intuition suggests that initial interaction of H with NO₂ occurs via the odd electron in this orbital. This is completely consistent with the purely attractive interaction (no activation barrier) observed for the entrance channel.

The justification for assuming planar symmetry in the correlation diagram is threefold. First, the entrance channel should favor planar reactive trajectories. Second, the HONO complex should also favor planar dynamics through the out-of-plane barrier at the minimum of the complex. Finally, the nonstatistical Λ -doublet production shows that the dissociation of the complex is preferentially planar.

Quantitative aspects of the energy and angular scattering distributions can only be explained when a quantitative potential surface is available. We do note, however, that the angular distribution is nearly statistical, while the energy is partitioned very nonstatistically. This again emphasizes that the lifetime of the complex is approximately the same as its rotational period, but that significantly longer times are required to fill all phase space and randomize energy partitioning. Similar behavior has also been observed in the reactions of fluorine atoms with olefins [26].

Our best guess concerning the limiting dynamics is as follows. As the hydrogen approaches the NO, it interacts principally with the electron in the planar sp² orbital on the nitrogen, and is immediately attracted. The hydrogen swings out towards an oxygen atom of NO, in some manner to form the HONO complex, primarily in the transplanar form. The exact trajectory is unclear. It may take $\approx 5 \times 10^{-12}$ s for the hydrogen to migrate from the nitrogen to the oxygen. Alternatively, this motion may be direct and fast, followed by several actual vibrational periods of the complex about its minimum geometry. In either case, the complex dissociates after $\approx 5 \times 10^{-12}$ s. Because of the barrier to internal rotation in HONO, the trajectory remains planar during dissociation. The NOH angle may open up somewhat along the minimum energy path for dissociation, which in turn could generate a torque on the OH fragment in the HONO plane and account for the large planar rotational excitation of OH that is observed. Since the N-OH bond must also lengthen during the reaction, this produces a rotation in the NO fragment in a countersense to that in OH. This is consistent with the observed rotation in NO and the antiparallel alignment of $\vec{J}_{\rm NO}$ relative to $\vec{J}_{\rm OH}$.

• $O(^{3}P) + C_{6}H_{12} \rightarrow OH + C_{6}H_{11}$

The technological importance of the reactions of O(³P) with hydrocarbons in areas such as combustion, air pollu-

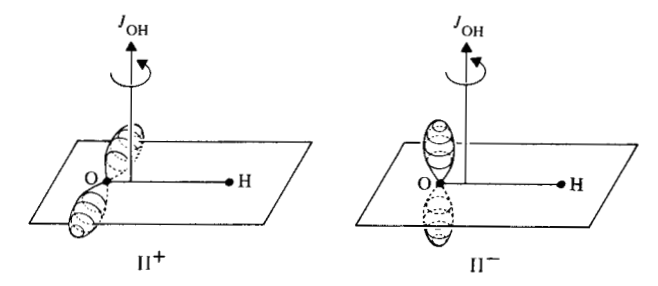


Figure 6 The physical difference between the two Λ -doublet components Π^+ and Π^- ; $J_{\rm OH}$ is the nuclear rotational angular momentum and the planes drawn are the planes of rotation of the molecule. The lobes about the oxygen atom represent the approximate electron density of the singly occupied OH π orbital.

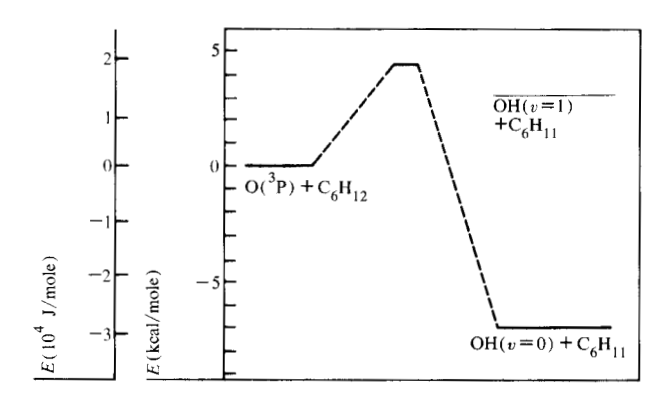


Figure 7 Schematic correlation diagram for the reaction $O(^3P) + C_6H_{12} \rightarrow OH + C_6H_{11}$.

tion, and atmospheric chemistry has spawned literally hundreds of measurements of thermal rate constants for use in kinetic models [27]. Despite this activity, even the identities of primary reaction products, *i.e.*, the *grossest* features of the reaction, have often remained speculative. There have been no studies of the dynamics of these reactions.

The kinetics of $O(^3P)$ reactions with saturated hydrocarbons RH are slow because of energy barriers of 3-8 kcal/mole (1-3 \times 10⁵ J/mole) [27]. It is generally assumed that the mechanism for these reactions involves a simple hydrogen abstraction:

$$O(^{3}P) + RH \rightarrow OH + R \cdot , \qquad (2)$$

where R •• is an alkyl radical. The correlation diagram for such a reaction with the saturated hydrocarbon cyclohexane is given in Fig. 7. The technique of crossed molecular beams with LIF detection of the OH product has confirmed this mechanism and has revealed many details of the reactive potential surface.

601

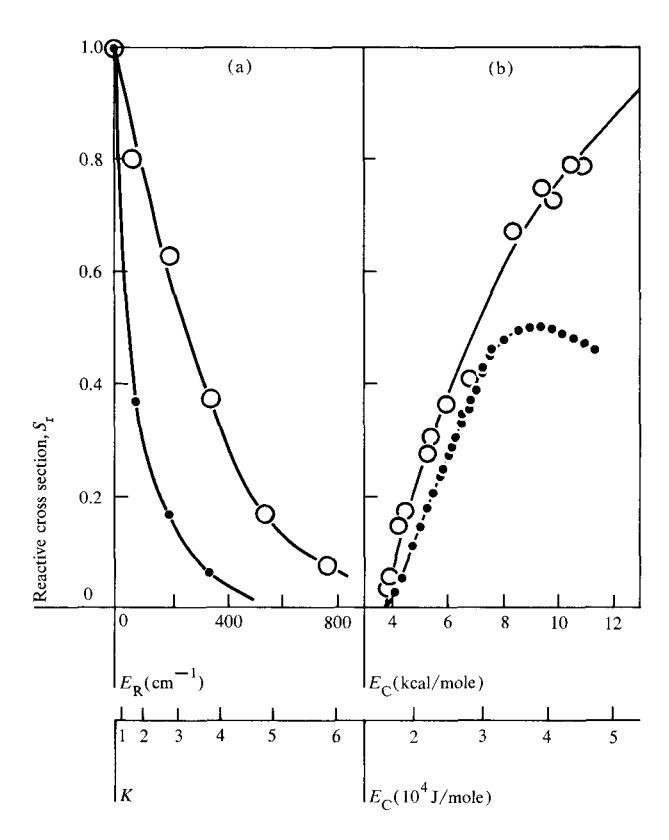


Figure 8 (a) Normalized rotational state distributions for the Π_1^+ fine structure component of the reaction $O(^3P) + C_eH_{12} \rightarrow OH + C_eH_{11}$. The lacklown indicate results for v=0 OH, the O, for v=1 OH; E_R is the rotational energy and K identifies the rotational quantum number. (b) Variation of some reactive cross sections S_r with center-of-mass collision energy E_C . The lacklown indicate results for the K=1, v=1 level, the O, for the K=1, v=0 level.

In these experiments an effusive beam of $O(^3P)$ at ≈ 300 K is generated by dissociation of O_2 in a microwave discharge. This beam is crossed by a supersonic nozzle beam of the hydrocarbon reactant seeded in H_2 or He. Velocities of the beams are measured from the time-of-flight values, and the relative density of RH in the seeded beam is monitored by modulated beam mass spectrometry as the conditions of this beam are varied. The initial center-of-mass collision energy is varied over the range 2-15 kcal/mole ($\approx 1-6 \times 10^5$ J/mole) by changing the temperature and the composition of the nozzle beam. The resolution in the center-of-mass collision energy is approximately ten percent.

The OH rotational state distribution for the reaction of $O(^{3}P) + C_{6}H_{12}$ is given in Fig. 8(a). In contrast to the result with the reaction of $H + NO_{2}$, there was only minimal excitation of OH rotation and this distribution was nearly

O(³P) with several other saturated hydrocarbons revealed that the OH rotational state distribution was identical within experimental limits for all such RH reactants.

The vibrational partitioning is obtained by summing each vibrational state over the respective rotational distribution. This yields $\sigma(v=0)/\sigma(v=1)=2.4$ at a collision energy of 10.5 kcal/mole (4.4 \times 10⁵ J/mole). This vibrational ratio is approximately independent of the hydrocarbon complexity as long as a *secondary* hydrogen is abstracted.

The variation of some of the reactive cross sections with collision energy is given in Fig. 8(b), which shows that the reaction occurs as a steeply rising function of the collision energy beyond some threshold value. The observed threshold value is slightly lower than but generally consistent with the activation energy obtained from the temperature dependence of the thermal rate constant [28]. The excitation function for v = 1 OH has a maximum, while that for v = 0 OH is a smoothly rising function. This also shows that the vibrational partitioning depends somewhat on the collision energy.

The independence with hydrocarbon complexity of the rotational and vibrational state distributions in the OH product suggests that the reaction dynamics are determined primarily by the properties of the C—H bond under attack, and not by properties of the entire molecule. This would imply that the internal modes of the R• product are not significantly excited during the reaction. Thus, a triatomic model for the reaction, where R• is treated as a structureless particle, may be appropriate and such a model should be general for reactions of O(³P) with all saturated hydrocarbons.

Rotational excitation in a reaction represents the torque that is generated on the product during the reactive collision. The extremely small rotational excitation in OH here implies that reaction occurs only when O(³P) approaches "colinearly" along a C—H bond and the OH also retreats colinearly. The minimal broadening of this distribution with collision energy also shows that the potential increases rapidly with the R—H—O angle.

Extensive classical scattering studies on model potential surfaces with barriers have yielded some generalizations about vibrational partitioning [29]. If the barrier is located in the entrance valley of the surface, the exothermicity of a reaction is released principally as vibrational excitation of the product. Conversely, if the barrier is in the exit channel, exothermicity is released principally as the relative translation of the separating particles. The results for the reaction of oxygen plus C_6H_{12} are be-

tween these two extremes, indicating a barrier about midway between the entrance and exit channels.

The variation of reactive cross sections with collision energy also appears very sensitive to variations in the potential surface [30], although the exact region of the surface that is most important is not yet clear. Current efforts are aimed at obtaining quantitative semi-empirical triatomic potential surfaces for the $O(^3P) + RH$ system, which, in conjunction with classical scattering calculations, will qualitatively describe the observed data. At present, a surface using the semi-empirical extended LEPS (London-Eyring-Polanyi-Sato) form [31] reproduces most of the observed features.

Conclusions

Two dissimilar reactions have been investigated by molecular beam LIF techniques and information has been obtained on their chemical dynamics and intermolecular potential surfaces. For $H + NO_2 \rightarrow OH + NO$, it appears that initial attack of the hydrogen is at the central atom of the triatomic molecule NO_2 , that the reaction is preferentially planar, and that the potential surface contains a deep well. For $O(^3P) + C_6H_{12} \rightarrow OH + C_6H_{11}$, the reaction occurs colinearly along a C-H bond and there is no well in the surface, but rather a barrier that occurs midway along the reaction coordinate.

Acknowledgments

The author wishes to acknowledge several coworkers who have collaborated in these experiments, especially P. Andresen, R. P. Mariella, Jr., and B. Lantzsch. The author also gratefully acknowledges V. T. Maxson for technical assistance, and R. K. Nesbet, W. A. Lester, Jr., and B. Liu for their many useful discussions.

References and notes

- 1. R. B. Bernstein, Israel J. Chem. 9, 615 (1971).
- J. M. Farrar and Y. T. Lee, in Annual Reviews of Physical Chemistry, Vol. 25, Annual Reviews, Inc., Palo Alto, CA, 1974, p. 357.
- A. Schultz, H. W. Cruse, and R. N. Zare, J. Chem. Phys. 57, 1354 (1972).
- R. P. Mariella, Jr., B. Lantzsch, V. T. Maxson, and A. C. Luntz, J. Chem. Phys. 69, 5411 (1978).
- R. A. Sutherland and R. A. Anderson, J. Chem. Phys. 58, 1226 (1973).
- For a review, see R. N. Zare and P. J. Dagdigian, Science 185, 739 (1974).
- 7. P. J. Dagdigian, Chem. Phys. 21, 453 (1977).
- A. Schultz, Fakultät für Physik der Universität, Hermann Herder-Str. 3, 78 Freiburg, W. Germany, private communication.
- 9. Z. Karny and R. N. Zare, J. Chem. Phys. 68, 3360 (1978).
- Z. Karny, R. C. Estler, and R. N. Zare, J. Chem. Phys. 69, 5199 (1978).
- J. B. Anderson, R. P. Andres, and J. B. Fenn, in Advances in Chemical Physics, Vol. 10, John Wiley & Sons, Inc., New York, 1966, p. 275.

- 12. G. S. Bahn, Reaction Rate Compilation for the H-O-N System, Gordon and Breach, New York, 1968.
- W. A. Guillory and C. E. Hunter, J. Chem. Phys. 54, 598 (1971).
- P. J. Robinson and K. A. Holbrook, Unimolecular Reactions, Wiley-Interscience, New York, 1972.
- 15. H. Haberland, R. Rohwer, and K. S. Schmidt, Chem. Phys. 5, 298 (1974). This reaction has recently been re-examined with simultaneous velocity and angular measurements of products, and much more accurate scattering distributions were obtained. Previous ambiguities in the laboratory to center-of-mass transformation have been eliminated. The newer center-of-mass scattering distribution is somewhat different from that published. H. Haberland, Facultät für Physik der Universität, Hermann Herder-Str. 3, 78 Freiburg, W. Germany, private communication.
- R. B. Bernstein and R. D. Levine, in Advances in Atomic and Molecular Physics, Vol. 11, D. R. Bates and B. Bederson, Eds., Academic Press, Inc., New York, 1975, p. 215.
- R. D. Levine and R. B. Bernstein, Chem. Phys. Lett. 22, 217 (1973).
- J. A. Silver, W. L. Dimpfl, J. H. Brophy, and J. L. Kinsey, J. Chem. Phys. 65, 1811 (1976).
- R. E. Smalley, B. L. Ramakrishna, D. H. Levy, and L. Wharton, J. Chem. Phys. 61, 4363 (1974).
- P. Pechukas, J. C. Light, and C. Rankin, J. Chem. Phys. 44, 794 (1966).
- The Π₁⁺, Π₁⁻, Π₂⁺, and Π₂⁻ fine structure components are the c, d, e, and f components, respectively, in more conventional notation; they correspond to the f₁, f₁', f₂, and f₂' components, respectively, in the notation of Crosswhite and Dieke. See H. M. Crosswhite and F. H. Dieke, J. Quant. Spect. Rad. Transfer 2, 97 (1962).
- R. P. Mariella, Jr. and A. C. Luntz, J. Chem. Phys. 67, 5398 (1977).
- 23. W. D. Gwinn, B. E. Turner, W. Miller Goss, and G. L. Blackman, Astrophys. J. 179, 789 (1973).
- 24. S. Green and R. N. Zare, Chem. Phys. 7, 62 (1975).
- C. F. Jackels and E. R. Davidson, J. Chem. Phys. 63, 4672 (1975).
- 26. J. M. Farrar and Y. T. Lee, J. Chem. Phys. 65, 1414 (1976).
- J. T. Herron and R. E. Huie, J. Phys. Chem. Ref. Data 2, 467 (1973).
- P. Kim and R. B. Timmons, Intl. J. Chem. Kinet. 7, 143 (1975).
- J. C. Polanyi and J. L. Schreiber, in *Physical Chemistry—An Advanced Treatise*, Vol. 6a, H. Eyring, W. Jost, and D. Henderson, Eds., Academic Press, Inc., New York, 1974, p. 383.
- M. Karplus, R. N. Porter, and R. D. Sharma, J. Chem. Phys. 43, 3259 (1965).
- P. J. Kuntz, in Modern Theoretical Chemistry, Vol. 2, Part B, W. H. Miller, Ed., Plenum Press, Inc., New York, 1976, p. 53.

Received March 1, 1979; revised March 26, 1979

The author is located at the IBM Research Division laboratory, 5600 Cottle Road, San Jose, California 95193.